

## Model calculation of local-field corrections to the static dielectric properties of a covalent semiconductor

Luiz E. Oliveira\*

*Department of Physics, University of California, Berkeley, California 94720  
and Materials and Molecular Research Division, Lawrence Berkeley Laboratory, Berkeley, California 94720*

J. d'Albuquerque e Castro

*Departamento de Física, Universidade Federal de São Carlos, São Carlos, SP 13560, Brazil  
(Received 8 April 1985)*

The wave-vector-dependent macroscopic response functions of diamond and silicon are calculated using a simple model for the static dielectric matrix of a covalent semiconductor. Local-field corrections are taken into account using a Wannier-function inversion technique in which the microscopic static dielectric response  $\epsilon_{\mathbf{G}\mathbf{G}'}^{-1}(\mathbf{q})$  is modeled by two mechanisms of screening, one corresponding to the response by a uniform homogeneous medium characterized by  $\epsilon_0(\mathbf{q}+\mathbf{G})$  and the other by a set of dipoles interacting via the screened electron-electron interaction  $v(\mathbf{q}+\mathbf{G})/\epsilon_0(\mathbf{q}+\mathbf{G})$ . Results for the static dielectric constant with and without local-field effects are compared to previous model calculations. The static microscopic dielectric response is tested in the long-wavelength limit via an analysis in real space of the microscopic local field and polarization charge density induced by a uniform externally applied electric field along the [111] direction.

### I. INTRODUCTION

The effects of local microscopic fields in the static dielectric response of semiconductors and insulators have been the subject of intensive theoretical work over the last few years.<sup>1-4</sup> Local-field effects essentially constitute a measure of the inhomogeneity of the system, and inclusion of these effects into the theory of microscopic dielectric screening in periodic solids leads to the definition<sup>5,6</sup> of a microscopic dielectric matrix  $\epsilon_{\mathbf{G},\mathbf{G}'}(\mathbf{q},\omega)$  in which  $\mathbf{G}$  and  $\mathbf{G}'$  are reciprocal-lattice vectors. In this paper we are mostly concerned with the static microscopic response  $\epsilon_{\mathbf{G},\mathbf{G}'}^{-1}(\mathbf{q})$  and the macroscopic dielectric function  $\epsilon_{\mathbf{M}}(\mathbf{q}) = 1/\epsilon_{\mathbf{0},\mathbf{0}}^{-1}(\mathbf{q})$ . The magnitude of the off-diagonal elements of  $\epsilon$  measures the contribution of local-field corrections to the microscopic response: A purely diagonal dielectric response matrix essentially corresponds to the response of a model homogeneous solid and is therefore unable to account for the changes in the microscopic electric field and polarization charge density caused by variations in the electronic environment on the scale of atomic dimensions.

The evaluation of the full dielectric response matrix of a periodic solid requires the previous knowledge of its electronic band structure and constitutes an extremely time-consuming calculation. For an arbitrary  $\mathbf{q}$  the polarization integrals have to be carried out over the full Brillouin zone (BZ) and need to be evaluated for every pair of  $\mathbf{G},\mathbf{G}'$  reciprocal-lattice vectors. Moreover, after the matrix elements  $\epsilon_{\mathbf{G},\mathbf{G}'}(\mathbf{q})$  are obtained, a full inversion is still required to obtain the microscopic response  $\epsilon^{-1}$ . As a result, in recent years a number of approximations and phenomenological models have been proposed in which one relies on simplified electronic band structures, high-

symmetry materials, and mean-point BZ averaging techniques. The resulting model dielectric matrices have been used in such important applications as lattice dynamics,<sup>4,7-9</sup> screening of impurities,<sup>3,10</sup> local-field studies in real space,<sup>1,2</sup> etc., and although the relative accuracy and reliability of the different model calculations have not yet been unambiguously established, the continuing development of physically simple models for the microscopic dielectric response of periodic solids is clearly of fundamental importance.

In this work a model calculation of the macroscopic dielectric response  $\epsilon_{\mathbf{M}}(\mathbf{q})$  for diamond and silicon is presented. The static dielectric constant with and without local-field effects is evaluated and results compared with previous model calculations. Moreover, the microscopic static dielectric response matrix  $\epsilon_{\mathbf{G},\mathbf{G}'}(\mathbf{q})$  is tested for  $\mathbf{q} \rightarrow \mathbf{0}$  with an analysis in real space of the microscopic local field and polarization charge density induced by a uniform externally applied electric field along the [111]-bond direction.

### II. THE MODEL MICROSCOPIC DIELECTRIC RESPONSE

The general form of the dielectric response matrix is<sup>5,6</sup>

$$\epsilon_{\mathbf{G},\mathbf{G}'}(\mathbf{q},\omega) = \delta_{\mathbf{G},\mathbf{G}'} - \frac{4\pi e^2}{|\mathbf{q}+\mathbf{G}| |\mathbf{q}+\mathbf{G}'|} \Pi_{\mathbf{G},\mathbf{G}'}(\mathbf{q},\omega), \quad (2.1)$$

where  $\Pi_{\mathbf{G},\mathbf{G}'}(\mathbf{q},\omega)$  is the polarizability. Within the random-phase approximation and within the Wannier-function factorization scheme, the polarizability is given by<sup>11,12</sup>

$$\Pi_{\mathbf{G},\mathbf{G}'}(\mathbf{q},\omega) = 2 \sum_{s,s'} A_s(\mathbf{q}+\mathbf{G}) N_{ss'}(\mathbf{q},\omega) A_{s'}^*(\mathbf{q}+\mathbf{G}'), \quad (2.2)$$

where  $A_s(\mathbf{q}+\mathbf{G})$  is a form factor between Wannier functions  $\phi_\nu(\mathbf{r})$  and  $\phi_\mu(\mathbf{r}+\mathbf{R}_l)$  and the index  $s$  stands for the lattice vector index  $l$  and for the indices  $\nu$  and  $\mu$  of the Wannier functions used to describe the Bloch functions. The matrix  $N_{ss'}(\mathbf{q},\omega)$  contains the Fermi factors and energy eigenvalues and each  $(s,s')$  term involves an integration over the Brillouin zone. Turner and Inkson<sup>13</sup> argued that the major contribution to the dielectric matrix comes from those terms with form factors  $A_s(\mathbf{q}+\mathbf{G})$  which correspond to both the bonding and antibonding orbitals centered on the same site and pointing in the same direction. Further, they proposed an extreme tight-binding approximation with a single effective gap  $E_g$  between conduction and valence bands. Within the approximations of Turner and Inkson,<sup>13</sup> the matrix  $\underline{N}$  is diagonal and the response matrix becomes

$$\epsilon_{\mathbf{G},\mathbf{G}'}(\mathbf{q},\omega) = \delta_{\mathbf{G},\mathbf{G}'} + \frac{4\pi e^2}{\Omega_c |\mathbf{q}+\mathbf{G}| |\mathbf{q}+\mathbf{G}'|} \left[ \frac{4E_g}{E_g^2 - \omega^2} \right] \times \sum_{\nu} A_\nu(\mathbf{q},\mathbf{G}) A_\nu^*(\mathbf{q},\mathbf{G}'), \quad (2.3)$$

where

$$A_\nu(\mathbf{q},\mathbf{G}) = e^{i\mathbf{G}\cdot\mathbf{d}} \int \phi_\nu^+(\mathbf{r}) e^{-i(\mathbf{q}+\mathbf{G})\cdot\mathbf{r}} \phi_\nu^-(\mathbf{r}) d\mathbf{r}, \quad \mathbf{d} = \frac{a}{8}(1,1,1) \quad (2.4)$$

is a form factor between bonding ( $\phi_\nu^+$ ) and antibonding ( $\phi_\nu^-$ ) wave functions,  $\Omega_c$  is the volume of the unit cell,  $a$  is the lattice parameter, and  $\nu$  denotes the four tetrahedral directions for a diamond-type semiconductor. As Turner and Inkson pointed out,<sup>13</sup> the above factorization ansatz for the polarizability overestimates the local-field corrections since it is strictly valid for tightly bound electrons only. We found, however, that a functional form similar to the one proposed by Turner and Inkson<sup>13</sup> gives fairly good results for the local-field corrections and has a simple physical interpretation. At the same time it retains the important property of making the  $\epsilon^{-1}$  dielectric response easily obtainable via the Wannier-function inver-

sion technique. Our factorization ansatz<sup>14</sup> for the static microscopic dielectric response is

$$\epsilon_{\mathbf{G},\mathbf{G}'}(\mathbf{q}) = \epsilon_0(\mathbf{q}+\mathbf{G}) \delta_{\mathbf{G},\mathbf{G}'} + \gamma \frac{4\pi e^2}{\Omega_c |\mathbf{q}+\mathbf{G}| |\mathbf{q}+\mathbf{G}'|} \left[ \frac{4}{E_g} \right] \times \sum_{\nu} A_\nu(\mathbf{q},\mathbf{G}) A_\nu^*(\mathbf{q},\mathbf{G}'), \quad (2.5)$$

which has a simple interpretation if one considers that in the Jones zone scheme,<sup>15</sup> as Inkson<sup>16</sup> suggested, there are basically two physically distinct types of contribution for the polarizability:

(a) The first type is a "surface" contribution which essentially comes from the region in  $k$  space around the Jones zone surface, i.e., the region around the principal band gap of the semiconductor. In that scheme, the off-diagonal elements, which reflect the nonhomogeneity of the electronic charge distribution, are dominated by what we called surface terms, and are expected to be fairly well represented within an extreme tight-binding model [the  $\gamma$  factor in (2.5) takes into account that only a fraction  $\gamma$  of the valence electrons contributes to the surface term].

(b) The second type is a "volume" term which comes from large regions of the "Fermi sea" with essentially free-electron-like behavior, and which gives no contribution to the off-diagonal elements of the dielectric matrix. For the diagonal elements  $\epsilon_{\mathbf{G},\mathbf{G}}(\mathbf{q})$ , on the other hand, we have contributions coming from both surface and metallic terms.

One should notice that the above factorization ansatz for  $\epsilon_{\mathbf{G},\mathbf{G}'}(\mathbf{q})$  can be related to the exact static Wannier procedure [Eqs. (2.1) and (2.2)] by taking  $\epsilon_0(\mathbf{q}+\mathbf{G}) \equiv 1$  and considering creation and annihilation of electron-hole pairs in different sites and different bonds conveniently weighted by the propagator  $N_{ss'}(\mathbf{q})$ . Physically what we have done was to approximate the Jones zone surface contribution by an extreme tight-binding term and substitute the smooth metalliclike volume contribution by a purely diagonal part  $\epsilon_0(\mathbf{q}+\mathbf{G})$ .

The separable form of the polarizability in (2.5) enables one to calculate easily<sup>11</sup> the inverse dielectric matrix

$$\epsilon_{\mathbf{G},\mathbf{G}'}^{-1}(\mathbf{q}) = \frac{1}{\epsilon_0(\mathbf{q}+\mathbf{G})} \left[ \delta_{\mathbf{G},\mathbf{G}'} - \gamma \frac{4\pi e^2}{\Omega_c |\mathbf{q}+\mathbf{G}| |\mathbf{q}+\mathbf{G}'|} \frac{4}{E_g} \frac{1}{\epsilon_0(\mathbf{q}+\mathbf{G}')} \sum_{\nu,\nu'} A_\nu(\mathbf{q},\mathbf{G}) S_{\nu\nu'}^{-1}(\mathbf{q}) A_{\nu'}^*(\mathbf{q},\mathbf{G}') \right], \quad (2.6)$$

with

$$S_{\nu\nu'}(\mathbf{q}) = \delta_{\nu\nu'} + \sum_{\mathbf{G}} \gamma \frac{4}{\Omega_c E_g} A_\nu^*(\mathbf{q},\mathbf{G}) \frac{4\pi e^2 / |\mathbf{q}+\mathbf{G}|^2}{\epsilon_0(\mathbf{q}+\mathbf{G})} A_{\nu'}(\mathbf{q},\mathbf{G}). \quad (2.7)$$

The static microscopic dielectric response  $\epsilon_{\mathbf{G},\mathbf{G}'}^{-1}(\mathbf{q})$  given above may be interpreted on physical grounds as being modeled by two mechanisms of screening corresponding to the responses by a uniform homogeneous medium characterized by  $\epsilon_0(\mathbf{q}+\mathbf{G})$  and by a set of dipoles

represented by the form factors  $A_\nu(\mathbf{q},\mathbf{G})$  interacting via the screened electron-electron interaction  $v(\mathbf{q}+\mathbf{G})/\epsilon_0(\mathbf{q}+\mathbf{G})$ . We should also stress that the proposed model has the advantage of being extremely simple from a computational point of view: The inversion of the infinite-

dimensional dielectric matrix  $\epsilon_{G,G'}(\mathbf{q})$  is reduced to the inversion of a simple  $4 \times 4$   $S_{\nu\nu}(\mathbf{q})$  matrix with indices corresponding to the four tetrahedral directions.

### III. RESULTS AND DISCUSSION

We have used the model static microscopic dielectric response  $\epsilon_{G,G'}(\mathbf{q})$  of Eq. (2.5) in calculating the macroscopic response

$$\epsilon_M(\mathbf{q}) = 1/\epsilon_{0,0}^{-1}(\mathbf{q}) \quad (3.1)$$

for diamond and silicon. We have chosen the origin midway between the two atoms in the [111] direction of the unit cell of diamond so that the form factors  $A_\nu(\mathbf{q},\mathbf{G})$  can be made real due to the inversion symmetry. We have used  $sp^3$ -hybridized orbitals localized in the four tetrahedral directions<sup>17</sup>

$$\Psi_\nu(\mathbf{r}) = (4\sqrt{\pi})^{-1} \left[ R_s(r) + \sqrt{3} \frac{\nu \cdot \mathbf{r}}{r} R_p(r) \right], \quad (3.2)$$

where  $\nu$  represents the tetrahedral vectors [111], [ $\bar{1}\bar{1}\bar{1}$ ], [ $\bar{1}\bar{1}1$ ], and [ $1\bar{1}\bar{1}$ ]. Two hybridized orbitals of nearest-neighbor atoms pointing in the same direction are added and subtracted to form<sup>17</sup> bonding  $\phi_\nu^+(\mathbf{r})$  and antibonding  $\phi_\nu^-(\mathbf{r})$  orbitals

$$\phi_\nu^\pm(\mathbf{r}) = [2(1 \pm S)]^{-1/2} \left[ \Psi_\nu(\mathbf{r}) \pm \Psi_{-\nu} \left( \mathbf{r} - \frac{a}{4}\nu \right) \right], \quad (3.3)$$

with  $S$  being the overlap<sup>17,18</sup> between  $\Psi_\nu(\mathbf{r})$  and  $\Psi_{-\nu}(\mathbf{r} - (a/4)\nu)$  [ $S(\text{diamond})=0.5$ ;  $S(\text{silicon})=0.7$ ]. We have taken the atomic  $s$  and  $p$  orbitals of diamond as hydrogenic orbitals<sup>13,14</sup> with an effective charge  $Z=2.5$ , while for those of silicon we have used a Gaussian expansion<sup>17</sup> optimized with respect to a current-conservation criterion and that also gives a reasonable fit to the charge density. With these choices the form factors are easily evaluated analytically. Further, for reciprocal-lattice vectors through the set (222) we have scaled<sup>19</sup>  $A_\nu(\mathbf{q},\mathbf{G})$  so that the contribution of the "surface" term to the diagonal matrix element  $\epsilon_{G,G}(\mathbf{q})$  corresponds to a fraction  $\gamma$  [cf. Eq. (2.5)] of the polarizability in the Penn model.<sup>15</sup> We have followed Penn's criterion<sup>15,16</sup> in choosing

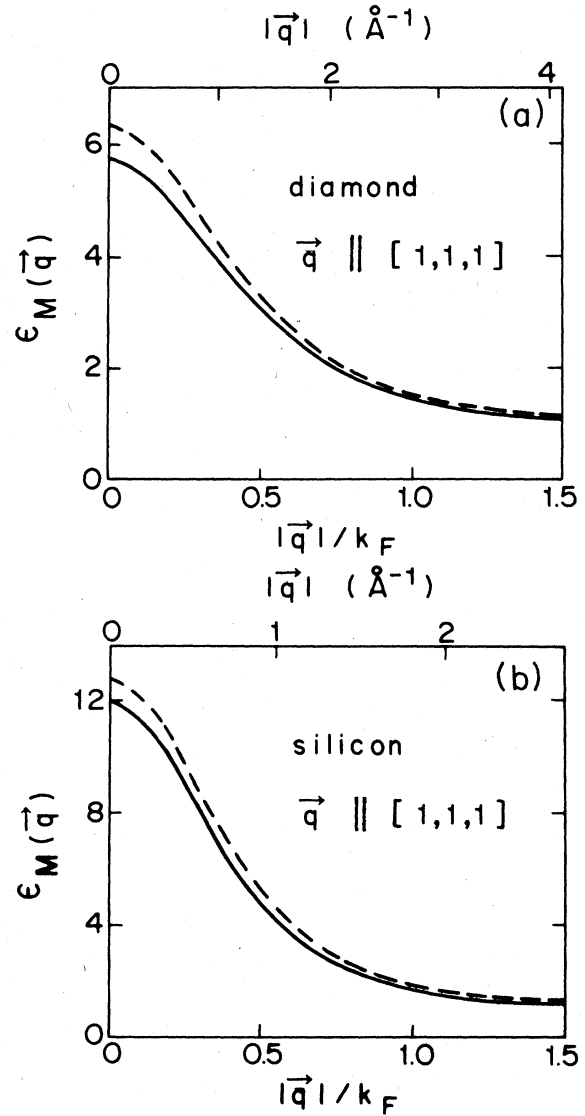


FIG. 1. Static macroscopic dielectric response  $\epsilon_M(\mathbf{q}) = 1/\epsilon_{0,0}^{-1}(\mathbf{q})$  for diamond and silicon along the [111] direction. Dashed curves correspond to diagonal terms only (no local-field effects); solid curves correspond to full matrix inversion (local-field effects are taken into account).

TABLE I. Anisotropy of the macroscopic static dielectric response  $\epsilon_M^{LF}(\mathbf{q})$ , including local-field effects, for diamond and silicon.

$q/k_F$	$\epsilon_M^{LF}(\mathbf{q})$ (diamond)			$\epsilon_M^{LF}(\mathbf{q})$ (silicon)		
	$q  [111]$	$q  [110]$	$q  [100]$	$q  [111]$	$q  [110]$	$q  [100]$
0.0	5.7	5.7	5.7	12.0	12.0	12.0
0.15	5.219	5.251	5.350	10.728	10.752	10.796
0.30	4.299	4.308	4.379	8.054	8.147	8.196
0.45	3.354	3.331	3.363	5.502	5.637	5.682
0.60	2.550	2.511	2.539	3.720	3.822	3.811
0.75	1.997	1.956	1.968	2.653	2.715	2.672
0.90	1.631	1.619	1.657	2.040	2.070	2.044
1.05	1.410	1.408	1.467	1.663	1.693	1.670
1.20	1.275	1.278	1.290	1.451	1.466	1.442
1.35	1.191	1.194	1.201	1.319	1.324	1.302
1.50	1.138	1.136	1.145	1.228	1.229	1.214

TABLE II. Comparison, in the case of diamond, of  $\epsilon_{\infty}^{\text{NLF}} = \lim_{q \rightarrow 0} \epsilon_{0,0}(\mathbf{q})$  (no local-field effects) and  $\epsilon_{\infty}^{\text{LF}} = \lim_{q \rightarrow 0} 1/\epsilon_{0,0}^{-1}(\mathbf{q})$  (local-field effects included) within different model calculations. The  $\delta$  parameter is defined as  $\delta = (\epsilon_{\infty}^{\text{LF}} - \epsilon_{\infty}^{\text{NLF}})/\epsilon_{\infty}^{\text{LF}}$ .

	$\epsilon_{\infty}^{\text{NLF}}$	$\epsilon_{\infty}^{\text{LF}}$	$\delta$
Van Vechten and Martin <sup>a</sup>	5.478	5.0	-9.6%
Johnson <sup>b</sup>	5.478	5.089	-7.6%
Van Camp <i>et al.</i> <sup>c</sup>	6.425	5.537	-16.0%
Turner and Inkson <sup>d</sup>	6.12	5.61	-9.1%
Baldereschi and Tosatti <sup>e</sup>	5.274	4.878	-8.1%
Mattausch <i>et al.</i> <sup>f</sup>	4.8	4.3	-11.6%
Present work	6.30	5.70	-10.5%

<sup>a</sup>See Ref. 20.

<sup>b</sup>See Ref. 21.

<sup>c</sup>See Ref. 8.

<sup>d</sup>See Ref. 13.

<sup>e</sup>See Ref. 22.

<sup>f</sup>See Ref. 3.

$\gamma = 3E_g/4E_F$  for the fraction of the valence electrons which, in our model, contributes to the surface term of the polarizability. Finally, we have determined the "volume" contribution  $\epsilon_0(\mathbf{q} + \mathbf{G})$  by imposing the condition that each diagonal element of the dielectric response matrix should reproduce the simple interpolation formula obtained by Penn,<sup>15</sup> and have fixed the value of the average band gap  $E_g$  ( $E_g = 12.8$  eV for diamond,  $E_g = 4.6$  eV for silicon) so that the long-wavelength dielectric constant  $\epsilon_{\infty}^{\text{LF}}$  including local-field corrections reproduces the experimental  $\epsilon_{\infty}^{\text{expt}}$  value [ $\epsilon_{\infty}^{\text{expt}}$ (diamond) = 5.7,  $\epsilon_{\infty}^{\text{expt}}$ (silicon) = 12].

Results of our model calculation of  $\epsilon_M(\mathbf{q})$  for diamond and silicon are shown in Fig. 1 for  $\mathbf{q}$  along the [111] direction. The solid curves correspond to the dielectric

TABLE III. Comparison, in the case of silicon, of  $\epsilon_{\infty}^{\text{NLF}} = \lim_{q \rightarrow 0} \epsilon_{0,0}(\mathbf{q})$  (no local field effects) and  $\epsilon_{\infty}^{\text{LF}} = \lim_{q \rightarrow 0} 1/\epsilon_{0,0}^{-1}(\mathbf{q})$  (local field effects included) within different model calculations. The  $\delta$  parameter is defined as  $\delta = (\epsilon_{\infty}^{\text{LF}} - \epsilon_{\infty}^{\text{NLF}})/\epsilon_{\infty}^{\text{LF}}$ .

	$\epsilon_{\infty}^{\text{NLF}}$	$\epsilon_{\infty}^{\text{LF}}$	$\delta$
Van Vechten and Martin <sup>a</sup>	12.05	10.76	-12.0%
Price <i>et al.</i> <sup>b</sup>	11.3	9.3	-21.5%
Louie <i>et al.</i> <sup>c</sup>	10.1	9.0	-12.2%
Turner and Inkson <sup>d</sup>	12.97	12.05	-7.6%
Baldereschi and Tosatti <sup>e</sup>	12.1	10.9	-11.0%
Van Camp <i>et al.</i> <sup>f</sup>	13.16	11.01	-19.5%
Hanke and Sham <sup>g</sup>	9.85	8.0	-23.1%
Mattausch <i>et al.</i> <sup>h</sup>	10.9	10.3	-5.8%
Present work	12.71	12.0	-5.9%

<sup>a</sup>See Ref. 20.

<sup>b</sup>See Ref. 7.

<sup>c</sup>See Ref. 23.

<sup>d</sup>See Ref. 13.

<sup>e</sup>See Ref. 22.

<sup>f</sup>See Ref. 24.

<sup>g</sup>See Ref. 17.

<sup>h</sup>See Ref. 3.

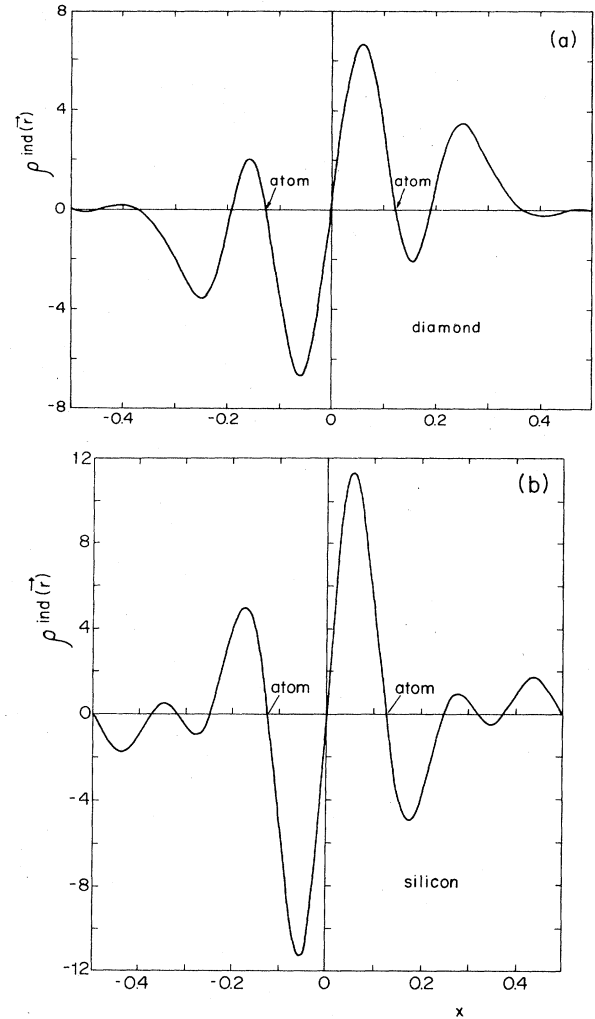


FIG. 2. Microscopic induced charge density  $\rho^{\text{ind}}(\mathbf{r})$ ,  $\mathbf{r} = a(x, x, x)$ , for diamond and silicon along the [111] direction and in units of electrons/unit cell. The polarization charge density  $\rho^{\text{ind}}(\mathbf{r})$  is induced by a constant displacement  $E^{\text{ext}} = 1$  a.u. parallel to the [111] direction.

responses including local-field effects [see Eq. (3.1)] while the dashed curves correspond to the diagonal responses  $\epsilon_{0,0}(\mathbf{q})$ ; i.e., no local-field effects are considered. The static macroscopic dielectric response was also evaluated for  $\mathbf{q}$  along the [100] and [110] directions and the anisotropy of the static response including local-field effects was found to be rather small (see Table I). In Tables II and III, our results for the long-wavelength static dielectric constant, both with  $\epsilon_{\infty}^{\text{LF}}$  and without  $\epsilon_{\infty}^{\text{NLF}}$  local-field corrections, of respectively, diamond and silicon are compared with some previous model calculations. The  $\delta$  parameter, defined as

$$\delta = (\epsilon_{\infty}^{\text{LF}} - \epsilon_{\infty}^{\text{NLF}})/\epsilon_{\infty}^{\text{LF}}, \quad (3.4)$$

and which constitutes a measure of the importance of local field corrections is also shown. Our results for  $\delta$  compare well with previous calculations for diamond, and with a recent calculation by Mattausch *et al.*,<sup>3</sup> in the case of silicon. The results in Tables II and III clearly reflect

the difficulties encountered by several investigators in modeling a realistic microscopic static dielectric response matrix.

Our present model for the static dielectric matrix was also tested in the long-wavelength limit via an analysis in real space of the local fields and polarization charges induced by a uniform externally applied electric field

$$\mathbf{E}^{\text{ext}}(\mathbf{r}) = E^{\text{ext}}(\mathbf{q}) \frac{\mathbf{q}}{|\mathbf{q}|} e^{i\mathbf{q}\cdot\mathbf{r}}, \quad \mathbf{q} \rightarrow 0 \quad (3.5)$$

along the [111] direction. The corresponding induced microscopic local field is given by<sup>14</sup>

$$\mathbf{E}(\mathbf{r}) = |\mathbf{E}^{\text{ext}}| \sum_{\mathbf{G}} \epsilon_{\mathbf{G},0}^{-1}(\mathbf{q}) \frac{\mathbf{q} + \mathbf{G}}{|\mathbf{q} + \mathbf{G}|} e^{i(\mathbf{q} + \mathbf{G})\cdot\mathbf{r}}, \quad \mathbf{q} \rightarrow 0 \quad (3.6)$$

while the polarization charge density induced by the uniform applied field is<sup>14</sup>

$$\rho^{\text{ind}}(\mathbf{r}) = \frac{i}{4\pi} E^{\text{ext}}(\mathbf{q}) \sum_{\mathbf{G}} |\mathbf{q} + \mathbf{G}| [\epsilon_{\mathbf{G},0}^{-1}(\mathbf{q}) - \delta_{\mathbf{G},0}] \times e^{i(\mathbf{q} + \mathbf{G})\cdot\mathbf{r}}, \quad \mathbf{q} \rightarrow 0. \quad (3.7)$$

In (3.6), the  $\mathbf{G}=0$  term gives the macroscopic field  $\mathbf{E}^{\text{ext}}\epsilon_{0,0}^{-1}(\mathbf{q})$  while the remaining terms yield the oscillations of the microscopic internal fields which fluctuate on the scale of the atoms involved rather than with the wavelength of the applied field.

One should note that the evaluation of either  $\mathbf{E}(\mathbf{r})$  or  $\rho^{\text{ind}}(\mathbf{r})$ , which depend on the  $\epsilon_{\mathbf{G},0}^{-1}(\mathbf{q})$  elements of the inverse dielectric matrix, provides a much more stringent test on a model dielectric response matrix than just the evaluation of the macroscopic dielectric response, which depends on a single  $\epsilon_{0,0}^{-1}(\mathbf{q})$  element.

Figure 2 shows our results for the microscopic induced polarization charge density  $\rho^{\text{ind}}(\mathbf{r})$  for  $\mathbf{r}$  along the [111] diagonal of the conventional unit cell. It is clear from Fig. 2 that strong and localized dipoles are induced on those [111] bonds which are parallel to the uniform ap-

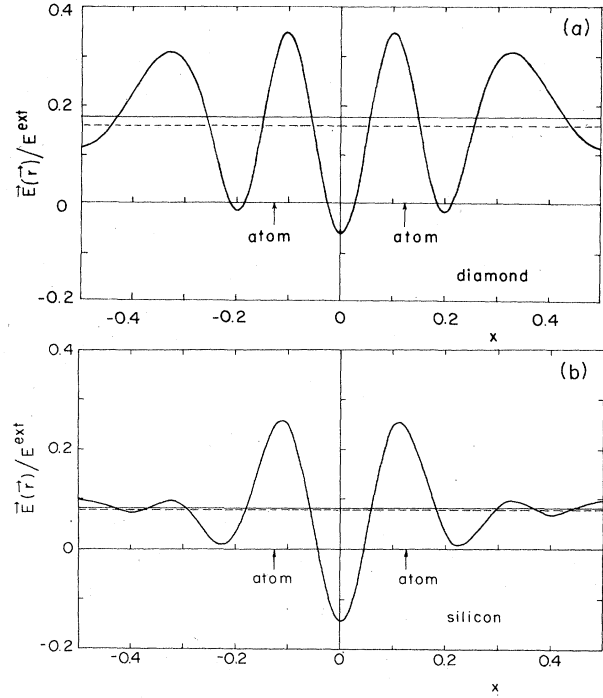


FIG. 3. Microscopic local field  $\mathbf{E}(\mathbf{r})$ ,  $\mathbf{r}=a(x,x,x)$ , for diamond and silicon along the [111] direction induced by a constant displacement  $\mathbf{E}^{\text{ext}}$  parallel to the [111] direction. Solid horizontal lines indicate the macroscopic field  $E^{\text{ext}}\epsilon_{0,0}^{-1}(\mathbf{q})$ ,  $\mathbf{q} \rightarrow 0$ , including local field corrections. Dashed horizontal lines correspond to the macroscopic field  $E^{\text{ext}}/\epsilon_{0,0}(\mathbf{q})$ ,  $\mathbf{q} \rightarrow 0$ , without local-field corrections.

plied electric field, as one would expect. The microscopic local field  $\mathbf{E}(\mathbf{r})$  induced by a uniform external field parallel to the [111] direction is shown in Fig. 3 for  $\mathbf{r}$  along the unit-cell [111] diagonal: The microscopic field fluctuates rather strongly in the unit cell and, at the bond center, the applied field is overscreened so that the microscopic local

TABLE IV. Some elements  $\epsilon_{\mathbf{G},0}^{-1}(\mathbf{q})$  of the inverse dielectric matrix for diamond and silicon in the limit  $\mathbf{q} \rightarrow 0$  along the [100] direction. Elements with  $|\mathbf{G}| < \sqrt{20} 2\pi/a$  which are not reported are related by symmetry or vanish. Also shown, for comparison, are the values obtained by Baldereschi, Car, and Tosatti (BCT) (Ref. 1).

$\mathbf{G}(a/2\pi)$	Diamond		Silicon	
	BCT <sup>a</sup>	This work	BCT <sup>a</sup>	This work
(000)	0.205	0.175	0.092	0.083
(111)	0.031	0.024	0.022	-0.003
(200)	0	0	0	0
(220)	-0.008	-0.017	-0.011	-0.015
(311)	-0.011	-0.010	-0.010	-0.010
(131)	-0.008	-0.011	-0.005	-0.007
(222)	-0.014	-0.010	-0.008	-0.005
(400)	-0.005	-0.002	-0.005	0.000
(133)	-0.001	-0.001	-0.001	-0.000
(313)	-0.002	0.000	-0.000	-0.000
(420)	0	0	0	0
(240)	0	0	0	0
(042)	-0.000	-0.001	-0.000	-0.000

<sup>a</sup>See Ref. 1.

field is in fact opposed to it. Results shown in Figs. 2 and 3 qualitatively agree with  $\mathbf{E}(\mathbf{r})$  and  $\rho^{\text{ind}}(\mathbf{r})$  obtained by Baldereschi *et al.*<sup>1</sup> Fairly good agreement is also obtained when the  $\epsilon_{\mathbf{G},0}^{-1}(\mathbf{q})$  elements,  $\mathbf{q} \rightarrow 0$  along the [100] direction, of our model dielectric response are compared with those obtained by Baldereschi *et al.*,<sup>1</sup> as shown in Table IV.

In conclusion, we have presented a model for the static dielectric matrix of diamond and silicon, which seems capable of realistically describing the static dielectric properties of these materials. Besides having a clear physical interpretation, this model is extremely simple from the computational point of view, and can be easily extended to the III-V semiconductors. It is also quite convenient for using in the study of several problems of current interest such as lattice dynamics and screening of impurities

in covalent semiconductors. Work along these lines is now in progress.

#### ACKNOWLEDGMENTS

This work was supported at the Lawrence Berkeley Laboratory by the Director of the Office of Energy Research, Office of Basic Energy Sciences, Materials Science Division of the Department of Energy, under Contract Number DE-AC03-76SF00098. In addition, the support of the U.S. National Science Foundation (through Grant NSF-INT83-12951) and the Brazilian Conselho Nacional de Desenvolvimento Científico e Tecnológico (CNPq) through their cooperative program is gratefully acknowledged. One of us (L.E.O.) would like to acknowledge the partial support of the Brazilian Government Agency Coordenação de Aperfeiçoamento de Pessoal do Ensino Superior (CAPES).

\*Permanent address: Instituto de Física, Unicamp, Campinas-SP, Brazil.

<sup>1</sup>A. Baldereschi, R. Car, and E. Tosatti, *Solid State Commun.* **32**, 757 (1979).

<sup>2</sup>K. Kunc and R. Resta, *Phys. Rev. Lett.* **51**, 686 (1983).

<sup>3</sup>H. J. Mattausch, W. Hanke, and G. Strinati, *Phys. Rev.* **27**, 3735 (1983).

<sup>4</sup>C. Falter, M. Selmke, W. Ludwig, and W. Zierau, *J. Phys. C* **17**, 21 (1984).

<sup>5</sup>S. L. Adler, *Phys. Rev.* **126**, 413 (1962).

<sup>6</sup>N. Wiser, *Phys. Rev.* **129**, 62 (1963).

<sup>7</sup>D. L. Price, S. K. Sinha, and R. P. Gupta, *Phys. Rev. B* **9**, 2573 (1974).

<sup>8</sup>P. E. Van Camp, V. E. Van Doren, and J. T. Devreese, *Phys. Rev. B* **17**, 2043 (1978).

<sup>9</sup>R. D. Turner and J. C. Inkson, *J. Phys. C* **11**, 3961 (1978).

<sup>10</sup>R. Car, A. Selloni, and M. Altarelli, *Solid State Commun.* **39**, 1013 (1981).

<sup>11</sup>W. R. Hanke, *Phys. Rev. B* **8**, 4585 (1973).

<sup>12</sup>H. Bilz, B. Gliss, and W. Hanke, *Dynamical Properties of Solids, Vol. 1*, edited by G. K. Horton and A. A. Maradudin (North-Holland, Amsterdam, 1974).

<sup>13</sup>R. D. Turner and J. C. Inkson, *J. Phys. C* **11**, 2875 (1978).

<sup>14</sup>L. E. Oliveira, *Phys. Status Solidi (B)* **107**, 255 (1981).

<sup>15</sup>D. R. Penn, *Phys. Rev.* **128**, 2093 (1962).

<sup>16</sup>J. C. Inkson, *J. Phys. C* **7**, 1571 (1974).

<sup>17</sup>W. Hanke and L. J. Sham, *Phys. Rev. B* **21**, 4656 (1980).

<sup>18</sup>J. N. Decarpigny and M. Lannoo, *Phys. Rev. B* **14**, 538 (1976).

<sup>19</sup>The essential motivation for that scaling is to make sure that the off-diagonal  $\epsilon_{\mathbf{G},\mathbf{G}'}(\mathbf{q})$  elements are evaluated with form factors which give diagonal  $\epsilon_{\mathbf{G},\mathbf{G}'}(\mathbf{q})$  elements with appropriate behavior. In a previous work for diamond (Ref. 14), this scaling was performed for  $\mathbf{G}$  vectors through the set (440), i.e.,  $|\mathbf{G}| \leq \sqrt{32} 2\pi/a$ , and results obtained were physically the same as in the present calculation for diamond.

<sup>20</sup>J. Van Vechten and R. Martin, *Phys. Rev. Lett.* **28**, 446 (1972).

<sup>21</sup>D. L. Johnson, *Phys. Rev. B* **9**, 4475 (1974).

<sup>22</sup>A. Baldereschi and E. Tosatti, *Phys. Rev. B* **17**, 4710 (1978).

<sup>23</sup>S. G. Louie, J. R. Chelikowsky, and M. L. Cohen, *Phys. Rev. Lett.* **34**, 155 (1975).

<sup>24</sup>P. E. Van Camp, V. E. Van Doren, and J. T. Devreese, *J. Phys. C* **12**, 3277 (1979).